

## Demonstration of Fusion-Evaporation and Direct-Interaction Nuclear Reactions using High-Intensity Laser-Plasma-Accelerated Ion Beams

P. McKenna,<sup>1,\*</sup> K. W. D. Ledingham,<sup>1,4</sup> T. McCanny,<sup>1</sup> R. P. Singhal,<sup>2</sup> I. Spencer,<sup>2</sup> M. I. K. Santala,<sup>3</sup> F. N. Beg,<sup>3</sup> K. Krushelnick,<sup>3</sup> M. Tatarakis,<sup>3</sup> M. S. Wei,<sup>3</sup> E. L. Clark,<sup>4</sup> R. J. Clarke,<sup>5</sup> K. L. Lancaster,<sup>5</sup> P. A. Norreys,<sup>5</sup> K. Spohr,<sup>6</sup> R. Chapman,<sup>6</sup> and M. Zepf<sup>7</sup>

<sup>1</sup>*Department of Physics, University of Strathclyde, Glasgow, G4 0NG, United Kingdom*

<sup>2</sup>*Department of Physics and Astronomy, University of Glasgow, Glasgow, G12 8QQ, United Kingdom*

<sup>3</sup>*Blackett Laboratory, Imperial College, London SW7 2BZ, United Kingdom*

<sup>4</sup>*Atomic Weapons Establishment, Aldermaston, Reading RG7 4PR, United Kingdom*

<sup>5</sup>*Central Laser Facility, Rutherford Appleton Laboratory, Chilton, Didcot, Oxon OX11 0QX, United Kingdom*

<sup>6</sup>*Department of Electronic Engineering and Physics, University of Paisley, Glasgow, PA1 2BE, United Kingdom*

<sup>7</sup>*School of Mathematics and Physics, Queen's University Belfast, Belfast BT7 1NN, United Kingdom*

(Received 16 January 2003; published 15 August 2003)

Heavy-ion induced nuclear reactions in materials exposed to energetic ions produced from high-intensity ( $\sim 5 \times 10^{19}$  W/cm<sup>2</sup>) laser-solid interactions have been experimentally investigated for the first time. Many of the radionuclides produced result from the creation of “compound nuclei” with the subsequent evaporation of proton, neutron, and alpha particles. Results are compared with previous measurements with monochromatic ion beams from a conventional accelerator. Measured nuclide yields are used to diagnose the acceleration of ions from laser-ablated plasma to energies greater than 100 MeV.

DOI: 10.1103/PhysRevLett.91.075006

PACS numbers: 52.70.Nc, 25.70.Gh, 25.70.Hi, 25.70.Jj

Recent investigations of plasmas produced from laser interactions with matter at intensities  $> 10^{19}$  W/cm<sup>2</sup> have shown that such plasmas can potentially be efficient sources of energetic electrons [1], gamma rays [2,3], and ions [4,5]. The acceleration of ions, in particular, has received a great deal of interest. During the interaction of laser radiation with a target foil proton fluxes ( $\sim 10^{12}$ ) are accelerated to energies up to tens of MeV and heavier ions to energies  $\sim 5$  MeV/nucleon. Constituent atoms at the surfaces of the target foil undergo field ionization and are accelerated in the direction normal to the surface by space-charge fields [6]. In addition, the presence of hydrocarbon and H<sub>2</sub>O contamination layers provide hydrogen, carbon, and oxygen, which are also ionized and accelerated.

There are many potential applications for the ions produced from these experiments, e.g., compact accelerators or as injectors for larger scale accelerators [7], as well as proton beams for fast ignition [8] and as a diagnostic probe beam of high density plasmas [9]. Promising medical applications have been highlighted, including laser-plasma driven ( $p, n$ ) and ( $p, \alpha$ ) reactions to produce short-lived isotopes for use in positron emission tomography (PET) [10].

Important physics in the laser-plasma based acceleration of electron and proton beams has been elucidated by systematic measurements of ( $\gamma, n$ ) and ( $p, n$ ) nuclear reactions [10–13]. However, measurements of heavy ion emission to date have been limited to Thomson parabola ion spectrometers, which generally sample small solid angles ( $\sim 10^{-5}$  sr) [14,6]. Consequently, they are not able to measure the integrated ion flux, given that the

ion expansion profile in some situations is influenced by self-generated electric and magnetic fields [14,15].

In this Letter we demonstrate for the first time that energetic “heavy ions,” accelerated in laser-ablated plasmas can induce nuclear reactions. It is shown that interactions of these fast ions with atoms in adjacent secondary “activation” targets create compound nuclei that deexcite through the evaporation of protons, neutrons, and alphas. High-resolution  $\gamma$ -ray spectra measured from nuclei in activated materials are obtained and used for the first time with calculated reaction cross sections to make quantitative measurements of ion emission. High-intensity laser-produced plasmas are shown to provide a source of heavy ions with a broad energy distribution, potentially important in the study of astrophysical nuclear reactions. In particular, high-intensity lasers are able to provide a quasithermal distribution of charged particles at typical astrophysical temperatures, which could be used to determine reaction rates to aid the understanding of stellar evolution [16].

This study was carried out using the chirped pulse amplified beam of the Vulcan Nd:glass laser. The wavelength was 1.054  $\mu$ m and pulse length was  $\sim 1$  ps. The  $p$ -polarized beam was focused using a 60 cm focal length parabolic mirror onto 100  $\mu$ m thick aluminum targets at an angle of 45° and to a peak intensity  $\sim 5 \times 10^{19}$  W/cm<sup>2</sup>. The target vacuum chamber was evacuated to  $< 10^{-4}$  mbar. Activation targets were exposed to the ion blow off from the front surface of the primary target foil. A well-shielded germanium detector (with a relative efficiency of 25% compared to the 3 in  $\times$  3 in NaI standard) was used to measure the characteristic gammas

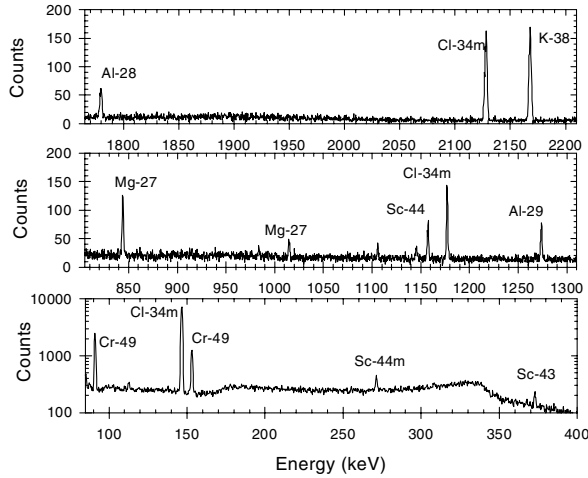


FIG. 1. Gamma-ray spectrum in an aluminum activation sample after irradiation with ions from an aluminum target foil.  $^{34m}\text{Cl}$ ,  $^{38}\text{K}$ ,  $^{28}\text{Al}$ ,  $^{29}\text{Al}$ ,  $^{24}\text{Na}$ ,  $^{27}\text{Mg}$ ,  $^{49}\text{Cr}$ ,  $^{43}\text{Sc}$ ,  $^{44}\text{Sc}$ , and  $^{44m}\text{Sc}$  peaks are observed.

emitted by the isotopes produced. Only nuclides with half-lives greater than a few minutes can be measured, as it requires about 10 min to remove the activated material from the target chamber. Nuclides were identified by the  $\gamma$  energies and half-lives.

In the first part of the experiment a 1 mm thick  $^{27}\text{Al}$  secondary sample was positioned along target normal direction, subtending a solid angle of  $\sim 4$  sr. After irradiation of the primary aluminum foil target with a 75 J laser pulse, characteristic peaks of  $^{34m}\text{Cl}$ ,  $^{38}\text{K}$ ,  $^{24}\text{Na}$ ,  $^{28}\text{Al}$ ,  $^{29}\text{Al}$ ,  $^{27}\text{Mg}$ ,  $^{49}\text{Cr}$ ,  $^{43}\text{Sc}$ ,  $^{44}\text{Sc}$ , and  $^{44m}\text{Sc}$  were measured in the  $^{27}\text{Al}$  activation sample; see Fig. 1. Table I lists the numbers of each nucleus determined after correction for detection efficiency and the gamma emission probability per disintegration, as well as possible production reactions.

Compound nuclear formation followed by particle evaporation (“fusion-evaporation”) is primarily respon-

sible for the production of the observed nuclei, although direct-interaction processes [17] are also likely. The Monte Carlo code PACE-2 [18] (projection angular-momentum coupled evaporation) was used to determine cross sections for the possible evaporation reactions. PACE-2 calculates the total fusion cross section for a projectile and target and incorporates atomic masses from the Audi/Wapstra tables [19] to compute the yields for fission exit channels. For each reaction process 10 000 fusion events were simulated in steps of 2 MeV to obtain the energy dependency plots shown in Fig. 2. The shape of the cross section for a fusion-evaporation reaction is generally found to be peaked for the most probable evaporation channel, with the high energy tail exhibiting different modes of decay resulting in the same nuclide (e.g.,  $^{34}\text{Cl}$  in Fig. 2). The estimated overall accuracy of the PACE-2 calculations is between 10% and 20%. The code could not be used to determine cross sections for the production of isomers and instead an experimental cross section [17] for  $^{34m}\text{Cl}$  was used. Reaction processes were identified based on the calculated cross sections and threshold energies.

The PACE-2 calculations indicate large cross sections for production of  $^{49}\text{Cr}$ ,  $^{43}\text{Sc}$ , and  $^{44}\text{Sc}$  by evaporation processes from the  $^{27}\text{Al} + ^{27}\text{Al}$  compound nucleus system (Table I).  $^{34m}\text{Cl}$ ,  $^{38}\text{K}$ ,  $^{24}\text{Na}$ ,  $^{28}\text{Al}$ ,  $^{29}\text{Al}$ , and  $^{27}\text{Mg}$ , however, are unlikely to result from  $^{27}\text{Al} + ^{27}\text{Al}$  compound reactions. The acceleration of contaminant carbon and oxygen ions to produce  $^{12}\text{C} + ^{27}\text{Al}$  and  $^{16}\text{O} + ^{27}\text{Al}$  reactions must be considered as pathways for the production of these nuclei. Similar nuclei were observed by Ladenbauer-Bellis *et al.* [17] using a monochromatic beam of 126 MeV  $^{12}\text{C}$  ions from a conventional accelerator incident on  $^{27}\text{Al}$  foil targets. Experimental cross sections and the PACE-2 calculations suggest that  $^{34m}\text{Cl}$  and  $^{38}\text{K}$  are formed via evaporation of alpha particles and neutrons from the  $^{12}\text{C} + ^{27}\text{Al}$  and  $^{16}\text{O} + ^{27}\text{Al}$  compound nucleus systems, but that  $^{24}\text{Na}$ ,  $^{28}\text{Al}$ ,  $^{29}\text{Al}$ , and  $^{27}\text{Mg}$  are unlikely to result from fusion-evaporation reactions.

TABLE I. The number of each nucleus induced per laser shot in the  $^{27}\text{Al}$  and  $^{12}\text{C}$  secondary samples. The most energetically favoured modes of decay of the compound nucleus systems  $^{27}\text{Al} + ^{27}\text{Al}$ ,  $^{12}\text{C} + ^{27}\text{Al}$  and  $^{16}\text{O} + ^{27}\text{Al}$  are considered as candidates for the production of these nuclei. The threshold energy,  $E_{\text{thresh}}$ , for each reaction is listed.

Observed nuclei	Half-life	Number of nuclei $N$		$^{27}\text{Al} + ^{27}\text{Al}$ Reactions	$E_{\text{thresh}}$ (MeV)	$^{12}\text{C} + ^{27}\text{Al}$ Reactions	$E_{\text{thresh}}$ (MeV)	$^{16}\text{O} + ^{27}\text{Al}$ Reactions	$E_{\text{thresh}}$ (MeV)
		$^{27}\text{Al}$ sample	$^{12}\text{C}$ sample						
$^{34m}\text{Cl}$	32.1 min	$2.8 \times 10^4$	$3.0 \times 10^4$	...	...	$^{34m}\text{Cl} + 1\alpha + 1n$	4.8	$^{34m}\text{Cl} + 2\alpha + 1n$	16.7
$^{38}\text{K}$	7.61 min	$1.7 \times 10^4$	$1.1 \times 10^3$	$^{38}\text{K} + 3\alpha + 3n + 1p$	87.9	$^{38}\text{K} + 1n$	...	$^{38}\text{K} + 1\alpha + 1n$	5.7
$^{28}\text{Al}$	2.24 min	$6.4 \times 10^4$	$4.6 \times 10^4$	...	...	$^{28}\text{Al} + 2\alpha + 2p + 1n$	39.9	$^{28}\text{Al} + 3\alpha + 2p + 1n$	55.7
$^{29}\text{Al}$	6.56 min	$4.5 \times 10^3$	$3.7 \times 10^3$	...	...	$^{29}\text{Al} + 2\alpha + 2p$	26.7	$^{29}\text{Al} + 3\alpha + 2p$	40.8
$^{24}\text{Na}$	14.98 h	$1.2 \times 10^4$	$9.2 \times 10^3$	...	...	$^{24}\text{Na} + 3\alpha + 2p + 1n$	56.2	$^{24}\text{Na} + 4\alpha + 2p + 1n$	73.0
$^{27}\text{Mg}$	9.46 min	$4.7 \times 10^3$	$1.4 \times 10^3$	...	...	$^{27}\text{Mg} + 2\alpha + 3p + 1n$	54.0	$^{27}\text{Mg} + 3\alpha + 3p + 1n$	71.0
$^{49}\text{Cr}$	41.9 min	$7.7 \times 10^3$	...	$^{49}\text{Cr} + 1\alpha + 1n$	...	...	...	...	...
$^{43}\text{Sc}$	3.89 h	$1.4 \times 10^4$	...	$^{43}\text{Sc} + 2\alpha + 1p + 2n$	52.5	...	...	$^{43}\text{Sc}$	...
$^{44}\text{Sc}$	3.93 h	$6.8 \times 10^3$	...	$^{44}\text{Sc} + 2\alpha + 1p + 1n$	30.0	...	...	...	...
$^{44m}\text{Sc}$	2.44 days	$7.3 \times 10^4$	...	$^{44m}\text{Sc} + 2\alpha + 1p + 1n$	...	...	...	...	...

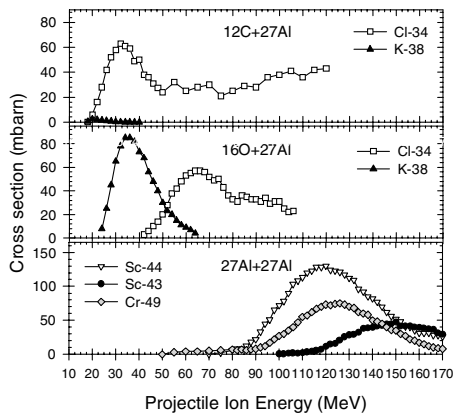


FIG. 2. Cross sections for the production of  $^{34}\text{Cl}$ ,  $^{38}\text{K}$ ,  $^{49}\text{Cr}$ ,  $^{43}\text{Sc}$ , and  $^{44}\text{Sc}$  calculated using the PACE-2 evaporation code for [ $^{12}\text{C} + ^{27}\text{Al}$ ], [ $^{16}\text{O} + ^{27}\text{Al}$ ], and [ $^{27}\text{Al} + ^{27}\text{Al}$ ] compound nucleus formation.

Ladenbauer-Bellis *et al.* attributed the production of  $^{24}\text{Na}$ ,  $^{29}\text{Al}$ , and  $^{27}\text{Mg}$  to direct interactions.

In a second experiment to highlight contributions arising from the acceleration of parasitic ions, a 1 mm thick  $^{12}\text{C}$  sample was used as the activation target and a  $^{27}\text{Al}$  target foil was irradiated with a 68 J laser pulse. Figure 3 shows that the characteristic gammas of  $^{34m}\text{Cl}$ ,  $^{38}\text{K}$ ,  $^{24}\text{Na}$ ,  $^{28}\text{Al}$ ,  $^{29}\text{Al}$ , and  $^{27}\text{Mg}$  are again observed and the numbers of each nucleus are listed in Table I.

The quantity of  $^{34m}\text{Cl}$ ,  $^{24}\text{Na}$ , and  $^{29}\text{Al}$  produced in both experiments agrees to within  $\pm 25\%$ , verifying that they originate via collisions between carbon and aluminum. The small variations may be due to the difference of  $\sim 10\%$  in the laser pulse energies and any shot-to-shot fluctuations. The larger yields of  $^{28}\text{Al}$  and  $^{27}\text{Mg}$  observed with the aluminum catcher target could result from the additional neutron-induced reaction channels  $^{27}\text{Al}(n, \gamma)^{28}\text{Al}$  and  $^{27}\text{Al}(n, p)^{27}\text{Mg}$ , not available with a carbon secondary target. A large difference (factor  $\sim 15$ )

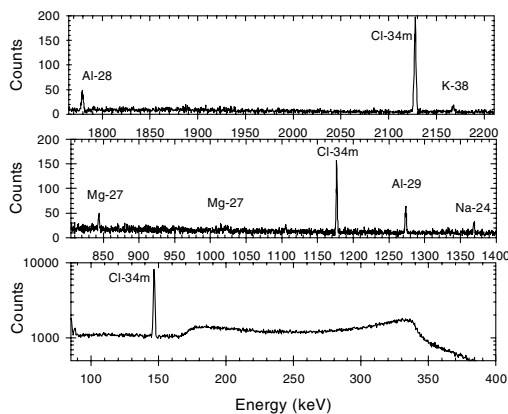


FIG. 3. Gamma-ray spectrum in a carbon activation sample after irradiation with ions from an aluminum target foil.  $^{34m}\text{Cl}$ ,  $^{38}\text{K}$ ,  $^{28}\text{Al}$ ,  $^{29}\text{Al}$ ,  $^{24}\text{Na}$ , and  $^{27}\text{Mg}$  peaks are observed.

in  $^{38}\text{K}$  is clearly seen when comparing the  $^{34m}\text{Cl}$  and  $^{38}\text{K}$  peaks at 2127 and 2167 keV, respectively, in Figs. 1 and 3. Although  $^{38}\text{K}$  can be produced from all three compound nucleus systems (Table I), PACE-2 calculations rule out the  $^{27}\text{Al} + ^{27}\text{Al}$  process, while indicating a relatively large cross section of the order of 85 mb at about 35 MeV for  $^{16}\text{O} + ^{27}\text{Al}$  (Fig. 2).

Nuclides for which the reaction process and mode of decay have been identified can be used to diagnose ion acceleration. This is possible because all of the ions are stopped in the activation target. Effectively the calculation involves a convolution of the cross section and the loss of energy as the ions propagate into the secondary target. The total number of each nuclide,  $N$ , produced for a given reaction is a product of the cross section  $\sigma(E)$ , the number of incident ions  $I(E)$ , the range of the ions in the activation target  $L(E)$ , and  $D$  the atom density in the activation target (where  $E$  is the ion energy). Although the energy distribution of observed heavy ions is unknown, the numbers of ions can be estimated using the peak cross section for each reaction. Effectively,  $I(E)$  corresponds to the number of ions with energy above the threshold energy for a reaction.  $L(E)$  was therefore obtained for the ion energy at the cross section peak minus the reaction threshold energy. SRIM-2003 [20], a Monte Carlo code that calculates the interactions of moving ions within matter using a quantum mechanical treatment of ion-atom collisions (from a few eV to 2 GeV) was used to determine the stopping ranges. The simulated collisions take into account a velocity dependent charge state of the moving ion and long range screening of the Coulomb potential by the target electrons (effective charge).

As illustrated in Fig. 4, about  $4 \times 10^9$  Al ions with energies of 50 and 33 MeV, respectively, are required to produce the observed quantities of  $^{34m}\text{Cl}$  and  $^{38}\text{K}$  in the carbon activation target. These values are similar to those determined using a Thomson parabola [7]. Using Gaf chromic film and CR-39 track detector it has been determined that the ions are emitted in a cone angle  $\sim 30^\circ$ ,

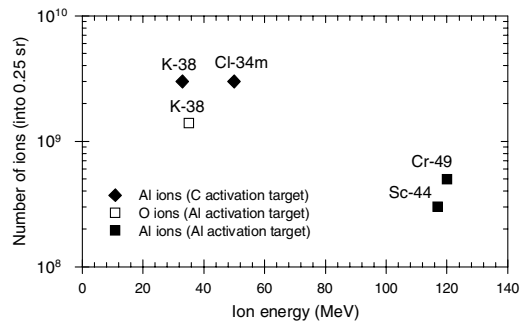


FIG. 4. Numbers of  $^{27}\text{Al}$  (closed symbols) and  $^{16}\text{O}$  (open symbol) ions, with energy above the reaction threshold energy, required to induce the measured activities of the nuclides indicated. Diamonds and squares correspond to carbon and aluminum activation samples, respectively.

with a corresponding solid angle of  $\sim 0.25$  sr. An order of magnitude less Al ions of higher energy,  $\sim 120$  MeV, are required for the production of  $^{49}\text{Cr}$  and  $^{44}\text{Sc}$  nuclei in the aluminum secondary target. Because of contributions from parasitic ions, the  $^{34m}\text{Cl}$  and  $^{43}\text{Sc}$  nuclei observed with this target were not unambiguously assigned to a particular compound reaction system (Table I) and therefore were not used in the determination of the ion spectra. It is interesting to note that the total conversion efficiency of laser energy to the *detected* fusion reactions via the acceleration of Al ions is of the order of 0.1%. As discussed above, the factor  $\sim 15$  increase in the production of  $^{38}\text{K}$  in the aluminum target is likely due to the  $^{16}\text{O} + ^{27}\text{Al}$  fusion-evaporation process. For the *additional*  $^{38}\text{K}$  nuclei to be produced via this reaction requires  $\sim 10^9$   $^{16}\text{O}$  ions. The increase in activity cannot be due to the reverse collision system, i.e.,  $^{27}\text{Al} + ^{16}\text{O}$ , as the oxygen contamination layer on the secondary target is insufficiently thick to account for the observed activity. The acceleration of oxygen ions from contamination layers on the primary target is expected, but has not been unambiguously identified using Thomson parabolas. The  $^{27}\text{Al}(n, p)^{27}\text{Mg}$  cross section, which has a peak of about 105 mb at 10 MeV, would require  $10^6$  neutrons/sr (assuming an isotropic distribution) to account for the *additional*  $^{27}\text{Mg}$  observed.

In summary, through the acceleration of ions in laser-produced plasmas, fusion-evaporation reactions have been induced in secondary targets for the first time and successfully used to diagnose heavy ion acceleration. Although the large distribution of ion energies typically produced is neglected, an indication of the numbers of ions involved in reactions with cross sections peaked in different regions of the ion energy spectrum is obtained. By inducing suitable reactions with cross sections peaked at high energies, this technique may become even more important in the diagnosis of ions produced with petawatt lasers. The technique benefits from the very large dynamic range and, as counting is off-line, insensitivity to electrical noise generated by the laser-plasma interaction. It is also possible to obtain angularly resolved measurements of energetic heavy ions by using “arrays” of catcher foils, and by using “stacked” catcher foils the reactions induced as a function of ion energy can be determined.

This work has initiated investigations using high-intensity lasers to provide large energy distributions of heavy ions for charged-particle-induced reactions, which are useful for the determination of astrophysical reaction rates. This initial study has shown that the range of reactions induced can be changed by the presence of surface contaminants highlighting the need for such experimentation to take place under controlled conditions, as in traditional nuclear physics. As the peak intensity of laser systems continues to increase, in the future such experiments may also prove to be an efficient method to produce unusual nuclear isotopes and isomers.

We acknowledge the assistance of the Vulcan operations team. P. M. gratefully acknowledges Royal Society of Edinburgh/SEELLD support.

---

\*Electronic mail: p.mckenna@phys.strath.ac.uk

- [1] V. Malka *et al.*, *Science* **298**, 1596 (2002).
- [2] M. H. Key *et al.*, *Phys. Plasmas* **5**, 1966 (1998).
- [3] M. I. K. Santala *et al.*, *Phys. Rev. Lett.* **84**, 1459 (2000).
- [4] E. L. Clark *et al.*, *Phys. Rev. Lett.* **84**, 670 (2000).
- [5] R. A. Snavely *et al.*, *Phys. Rev. Lett.* **85**, 2945 (2000).
- [6] M. Hegelich *et al.*, *Phys. Rev. Lett.* **89**, 085002 (2002).
- [7] K. Krushelnick *et al.*, *IEEE Trans. Plasma Sci.* **28**, 1184 (2000).
- [8] M. Roth *et al.*, *Phys. Rev. Lett.* **86**, 436 (2001).
- [9] M. Borghesi *et al.*, *Phys. Rev. Lett.* **88**, 135002 (2002).
- [10] I. Spencer *et al.*, *Nucl. Instrum. Methods Phys. Res., Sect. B* **183**, 449 (2001).
- [11] K. W. D. Ledingham *et al.*, *Phys. Rev. Lett.* **84**, 899 (2000).
- [12] T. E. Cowan *et al.*, *Phys. Rev. Lett.* **84**, 903 (2000).
- [13] M. I. K. Santala *et al.*, *Phys. Rev. Lett.* **86**, 1227 (2001).
- [14] E. L. Clark *et al.*, *Phys. Rev. Lett.* **85**, 1654 (2000).
- [15] M. Tatarakis *et al.*, *Phys. Rev. Lett.* **81**, 999 (1998).
- [16] P. Mohr *et al.*, *Phys. Lett. B* **488**, 127 (2000).
- [17] I.-M. Ladenbauer-Bellis, I. L. Preiss, and C. E. Anderson, *Phys. Rev.* **125**, 606 (1962).
- [18] A. Gavron, *Phys. Rev. C* **21**, 230 (1980).
- [19] G. Audi and A. H. Wapstra, *Nucl. Phys.* **A595**, 409 (1995).
- [20] J. F. Ziegler, J. P. Biersack, and U. Littmark, *The Stopping and Ranges of Ions in Solids* (Pergamon Press, New York, 1985).